

Propagation of Taylor Vortex Fronts into Unstable Circular Couette Flow

M. Lücke,^(a) M. Mihelcic, and K. Wingerath

Institut für Festkörperforschung der Kernforschungsanlage Jülich, D-5170 Jülich, West Germany

(Received 31 October 1983)

Explicit finite-difference numerical solutions of the time-dependent Navier-Stokes equations for axisymmetric flow between concentric cylinders are presented for propagating Taylor vortex fronts. They are a prototype example for the expansion of a periodic pattern into regions occupied by an unstable homogeneous basic state—here circular Couette flow. The propagation speed and the evolution of the periodic state behind the front are determined quantitatively as functions of Reynolds number for systems with three different radius ratios.

PACS numbers: 47.20.+m, 05.70.Ln

The growth of a spatially periodic structure into a region occupied by an unstable homogeneous state has recently been investigated in various systems.¹⁻³ The main interest is not in the slow exponential growth of, e.g., spontaneous infinitesimal disturbances of the unstable basic state but rather in the fast expansion of a large disturbance consisting, e.g., of a (localized) region that contains already the periodic state. In this case it was shown⁴ for some model systems⁴⁻⁷ that the boundary or front between the two states propagates with a unique velocity into the region containing the unstable state. Furthermore, there are hints that the wavelength of the periodic pattern might be uniquely selected by the propagating front.^{6,7} To investigate these questions in quantitative detail in a real system we numerically simulated rotationally symmetric flows of an incompressible fluid of kinematic viscosity ν between concentric cylinders of three radius ratios $\eta = r_1/r_2 = 0.5066, 0.75,$ and 0.893 . Always the inner cylinder (radius r_1) was rotating and the outer one (radius r_2) was at rest. We solved the Navier-Stokes equations with an explicit finite-difference method^{8,9} on an isotropic grid of mesh size $0.05d$ with a time step $\Delta t \approx 0.003\tau$. Here $\tau = d^2/2\pi\nu$ measures the characteristic time for diffusing momentum across the gap $d = r_2 - r_1$.

In this driven dissipative system the "large disturbance" from which the periodic Taylor-vortex-flow (TVF) state grows consists of Ekman vortices. They are always present near a rigid non-rotating end plate bounding the fluid. However, if the reduced Reynolds number $\epsilon = R/R_c - 1$ is sufficiently far below the critical one¹⁰ for onset of TVF the vortex intensity falls off¹¹ rapidly towards the bulk occupied by the circular-Couette-flow (CCF) state with translational symmetry in the z direction. Propagating TVF fronts were generated in two ways: (i) In analogy to the pro-

cedure of Ahlers and Cannell¹ a stationary CCF state was established in the bulk with subcritical driving. Thereafter the driving was instantaneously stepped up to be supercritical at $\epsilon_0 > 0$. (ii) The inner cylinder was started from rest to the supercritical rotation rate. For the driving range $0.01 \leq \epsilon_0 \leq 0.1$ explored in this work we found that in both cases CCF appropriate to ϵ_0 is formed in the bulk of the annulus within two or three τ after the last step¹² (infinitesimal local inhomogeneities that eventually would destroy the unstable CCF if there were no propagating TVF front grow much more slowly¹²). Within that time also the first Ekman vortices are formed in procedure (ii). Thereafter the front propagation is similar in both cases,¹² but with the TVF front of (i) starting further away from a plate because of the extended Ekman vortex system established prior to the last step. In order to have a long propagation path we suppress the generation of Ekman vortices at the lower end, $z = 0$, of the annulus by imposing CCF boundary conditions there with subcritical driving, $\epsilon(z = 0) = -\epsilon_0$. Then we let the driving $\epsilon(z)$ increase very smoothly in the range $0 \leq z \leq 12d$ to join with vanishing derivative to a supercritical plateau, $\epsilon(z \geq 12d) = \epsilon_0$, extending up to the top plate at $25d$.

Figure 1 shows typical radial velocity fields $u(z)$ in the middle of the gap at successive times. Other velocity components and the pressure behave similarly. Furthermore, velocity profiles $u(z, t)$ at different radial positions r are practically identical up to a scale factor depending on r . Hence the plane of the TVF front moves at right angles to the cylinder walls downwards from the upper plate.

To monitor the evolution of the front, i.e., its velocity and shape, we determined positions $z_\alpha(t)$ where the TVF reaches the fraction α of the maximal bulk outflow intensity u_{max} (discarding the

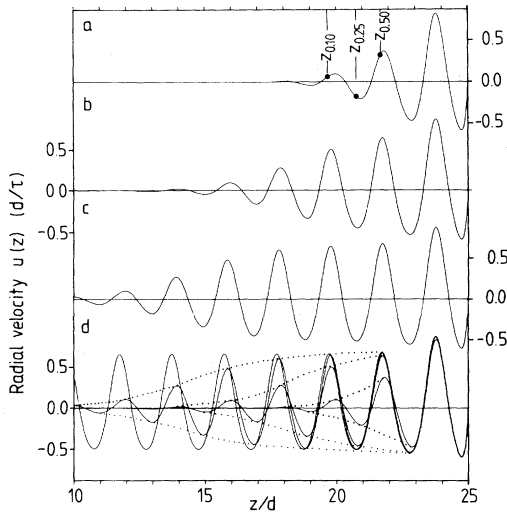


FIG. 1. Radial velocity fields $u(z)$ in the middle of the gap at times (a) 9.3τ , (b) 18.5τ , and (c) 27.8τ . ($\eta = 0.893$; $\epsilon_0 = 0.04$). (d) Shows the fields of (a)–(c) together with that at time $t = 90\tau$. Positive u implies outflow. Only the upper part of the annulus is shown. Dotted lines are guides to the eye. Dots in (a) denote front positions z_α of the intensity level αu_{\max} .

first two maxima near the top plate). The so-defined front positions move piecewise continuously. The discontinuity occurs whenever the intensity of the vortex just ahead of $z_\alpha(t)$ has grown up to αu_{\max} . Then the solution $z_\alpha(t)$ of $|u(z, t)| = \alpha u_{\max}$ jumps forward by about a vortex diameter. Figure 2 shows how far three different front intensity levels [dots in Fig. 1(a)] have traveled at successive discrete times since the step to supercritical driving. Obviously the periodic TVF state expands after some initial variation with a velocity c that is uniform in time behind a front with a time-invariant shape: The distances between different intensity levels are time independent, e.g., $z_{0.5}(t) - z_{0.1}(t) \approx 3.2d$. The front extension measured by these distances does, however, depend on the driving. For larger (smaller) ϵ_0 the above distance decreases (increases) and the front becomes sharper (less sharp).¹² Furthermore, the front extension decreases with the radius ratio η of the cylinders.¹²

Note that the propagation velocity of our largest intensity level ($0.5u_{\max}$) shown in Fig. 2 starts out to be markedly below the final velocity. Furthermore, it takes longest to reach stationarity while the propagation velocity of our smallest intensity level ($0.1u_{\max}$) approaches most rapidly the final value. This is so for all ϵ_0 and η . Therefore experiments which determine the TVF

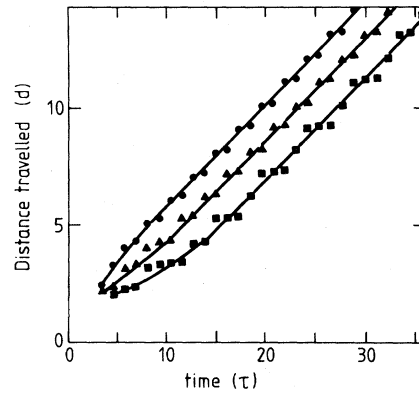


FIG. 2. Distance that the intensity levels αu_{\max} (cf. dots in Fig. 1) have traveled since step to supercritical driving $\epsilon_0 = 0.04$. Front positions marked by dots ($\alpha = 0.1$), triangles ($\alpha = 0.25$), and squares ($\alpha = 0.5$) were measured every 1.16τ . Lines are guides to the eye.

arrival time at a high intensity level only are susceptible to measuring too small early-stage velocities if the stationarity of the propagation velocity is not checked.

Figure 3 shows propagation velocities c of TVF fronts between cylinders of three different radius ratios for various driving in the range $0.01 \leq \epsilon_0 \leq 0.1$. Therein c varies in accordance with experiments¹ roughly proportional to $\sqrt{\epsilon_0}$. Note, however, the small systematic deviation from this power-law behavior. In contrast to the results of Ahlers and Cannell for $\eta = 0.893$ (open circles) our velocities lie for all our cylinders

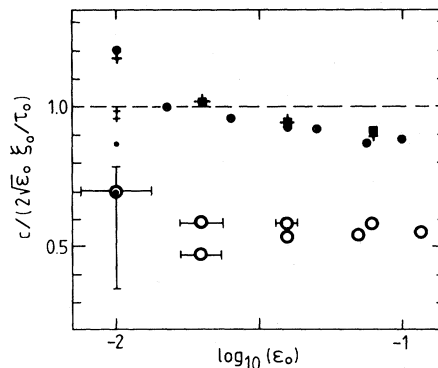


FIG. 3. Propagation velocities of TVF fronts between cylinders with radius ratio 0.5066 (dots), 0.75 (squares), and 0.893 (crosses) as a function of driving. See text for explanation of the small dots and crosses at $\epsilon_0 = 0.01$. The dashed line represents the result of the amplitude equation (1). Open circles are velocities reported in Ref. 1 for $\eta = 0.893$.

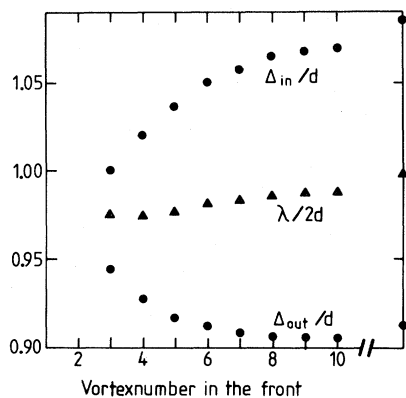


FIG. 4. Structure of the periodic state ($\eta=0.893$, $\epsilon_0=0.04$) unfolded by the front. Inflow and outflow intervals, Δ_{in} and Δ_{out} , are determined by the distance between successive nodes of $u(z)$. Numbering starts from the position $z_{0,1}$ of the intensity level $0.1u_{max}$. Triangles denote half the local wavelength $\lambda = \Delta_{in} + \Delta_{out}$ in the front. Bulk values behind the front are shown on the right boundary of the figure.

much closer to the unique front velocity $c = 2\epsilon_0^{1/2}\xi_0/\tau_0$ (dashed line) obtained^{4, 6} from

$$\tau_0 \partial_t A = (\xi_0^2 \partial_z^2 + \epsilon_0 - |A|^2/A_0^2)A. \quad (1)$$

Such equations¹³ for the slowly varying amplitude A of the periodic state represented by a stream function of the form $\psi = \text{Re}[A \exp(i 2\pi z/\lambda_0)]$ are thought to describe properly dissipative driven systems in the limit $\epsilon_0 \rightarrow 0$. The scales ξ_0 and τ_0 follow from linear stability analysis. They depend for the TVF instability weakly on η . In our η range ξ_0/τ_0 varies by less than 1% ($\xi_0/\tau_0 = 1.13d/\tau$ for $\eta = 0.893$).^{11, 14} The propagation velocities c for our three radius ratios coincide within (1–2)%. For the smallest driving our propagation velocities $c_{0.25}$ and $c_{0.5}$ of the larger intensity levels $0.25u_{max}$ and $0.5u_{max}$ were not yet stationary. (Propagation velocities slow down and front extensions increase with decreasing ϵ_0 !) We therefore included their values by small symbols—upper ones for $c_{0.25}$ and lower ones for $c_{0.5}$. In all other cases $c_{0.1} = c_{0.25} = c_{0.5} = c$ was stationary.

We finally address the problem of pattern selection by the propagating front. Figure 1(d) clearly shows that the nodes of $u(z, t)$ are not fixed but slowly move towards their final stationary positions after the front passes by. Hence flow pattern and local wavelength λ vary along the front and differ from the bulk. To elucidate the pattern evolution further Fig. 4 shows the distances between successive nodes of the radial velocity

field behind the moving front. First of all, since outflow away from the moving inner cylinder is faster than inflow the size Δ_{out} of the outflow domains are by mass conversion narrower than Δ_{in} . With growing intensity of the TVF these differences grow. That explains the decrease of Δ_{out} and the increase of Δ_{in} behind the front. Similarly, mass conservation seems to be the underlying mechanism for the variation of the flow pattern we observed¹² with driving: With increasing (decreasing) ϵ_0 the ratio Δ_{out}/Δ_{in} decreases (increases).

Because of the drastic variation of the node distances Δ_{in} and Δ_{out} in the front the spatial pattern of the “periodic” state varies considerably near the front even though the local wavelength varies only mildly in Fig. 4. Such a complicated spatial pattern evolution behind a propagating front cannot be reproduced by the above cited stream function [even if one were to replace λ_0 by some $\lambda(z - ct)$ to account for the wavelength variation propagating with the front] and an amplitude A solving (1). Lastly we mention that the spatial pattern of TVF near the front and in the bulk depends on the radius ratio. For example for $\eta = 0.5066$ inflow and outflow domains and the (local) wavelengths are smaller by about (2–3)%.¹²

(a)Permanent address: Fachrichtung Theoretische Physik, Universität des Saarlandes, D-6600 Saarbrücken, West Germany.

¹G. Ahlers and D. S. Cannell, Phys. Rev. Lett. **50**, 1583 (1983).

²J. S. Langer, Rev. Mod. Phys. **52**, 1 (1980).

³G. I. Sivashinsky, “Instabilities, Pattern Formation, and Turbulence in Flames” (to be published).

⁴D. G. Aronson and H. F. Weinberger, *Advances in Mathematics* (Academic, New York, 1978), Vol. 30, p. 33.

⁵E. Coutsias and B. A. Huberman, Phys. Rev. B **24**, 2592 (1981).

⁶G. Dee and J. S. Langer, Phys. Rev. Lett. **50**, 383 (1983).

⁷J. S. Langer and H. Müller-Krumbhaar, Phys. Rev. A **27**, 499 (1983).

⁸M. Lücke, M. Mihelcic, K. Wingerath, and G. Pfister, J. Fluid Mech. (to be published).

⁹J. E. Welch, F. H. Harlow, J. P. Shannon, and B. J. Daly, Los Alamos Scientific Laboratory Report No. LA-3425, 1966 (unpublished).

¹⁰R. C. Di Prima and H. L. Swinney, in *Hydrodynamic*

Instabilities and the Transition to Turbulence, edited by H. L. Swinney and J. P. Gollub (Springer, Berlin, 1981).

¹¹G. Pfister and I. Rehberg, *Phys. Lett.* 83A, 19 (1981).

¹²M. Lücke, M. Mihelcic, and K. Wingerath, to be

published.

¹³L. A. Segel, *J. Fluid Mech.* 38, 203 (1969); A. C. Newell and J. A. Whitehead, *J. Fluid Mech.* 38, 279 (1969).

¹⁴R. W. Graham and J. A. Domaradzki, *Phys. Rev. A* 26, 1572 (1982).